From Darkness to Light
ASP Conference Series, Vol. 3×10^8*, 2000*
T. Montmerle & Ph. André, eds.

Overview of Cluster Properties

Bruce A. Wilking

University of Missouri-St. Louis, Department of Physics & Astronomy, St. Louis, MO U.S.A. 63121

Abstract. Due in large part to advances of infrared arrays, the importance of the cluster mode of star formation in giant molecular clouds has been revealed. Because of the wide range of evolutionary states displayed by young low-mass stars, observations of young clusters at x-ray, visible, infrared, millimeter, and radio wavelengths are necessary to obtain a complete census of the cluster membership. From these data, the stellar density, frequency of circumstellar disks, and binary frequency in young clusters can be determined. By combining optical and infrared spectroscopy with photometry and pre-main sequence evolutionary models, the age and mass distributions within a cluster can also be investigated. In this review, the observable properties of young clusters will be summarized with emphasis on clusters within 1 kpc of the Sun. The mass functions of young clusters down to the hydrogen-burning limit will be compared with each other and with the field star Initial Mass Function. Finally, the ultimate fate of these young clusters, once free of their associated molecular gas, will be discussed.

Key words: stellar densities, disk frequency, binary frequency, age and mass distributions, bound clusters

1. Introduction

It is only in the last decade that the importance of the cluster mode of star formation has been realized in molecular clouds in the solar neighborhood. In the Orion giant molecular cloud (GMC), an extensive near-infrared survey of the L1630 region has revealed three rich clusters: NGC 2024, NGC 2068, and NGC 2071 (E. Lada et al. 1991). Considering deeper near-infrared surveys plus x-ray, Hα and IRAS surveys, it is estimated that 60%–90% of young stellar objects (YSOs) in the L1630 cloud with M>1 $M_\odot$ and formed in the last 10 Myr lie in these rich clusters (Meyer & E. Lada 1999; Li, Evans, & E. Lada 1997). Similarly, it is estimated that >66% of YSOs in the L1641 branch of the Orion GMC formed in the last 10 Myr are in dense clusters or aggregates if the clusters OMC-1 and 2 are included.

In this contribution, I will review the properties of clusters of pre-main sequence (PMS) stars with ages less than 10 Myr and within 1 kpc of the Sun. The variety of observations that establish the membership of young clusters, the observational properties of young clusters, and their inferred distributions of ages and masses will be summarized. The evolution of cluster properties and their ultimate fate will also be discussed. For this discussion, I will use the definition of a cluster given by Lada & Lada (1991) as a group of 10 or more physically related stars whose surface density significantly exceeds that of the field for stars of the same type. To be stable against tidal disruption from passing interstellar clouds, the stellar mass density must exceed 1 $M_\odot$ pc^{-3} (Spitzer 1958). Young clusters can be classified on the basis of the degree of association with molecular gas, whether or not they are gravitationally bound, and richness. It is observed that clusters maintain an association with a significant amount of molecular gas until an age of ~10 Myr (Leisawitz, Bash, & Thaddeus 1989). In that sense, the clusters considered here are still embedded and, due in large part to their association with molecular gas, gravitationally bound.

There is a continuum in the richness among young clusters ranging from relatively poor clusters (or aggregates) containing 10–20 stars to rich clusters such as the Orion Nebula Cluster (ONC) containing thousands of stars. There is some physical basis for distinguishing between an aggregate and a rich cluster. Since the time needed to collisionally relax a cluster scales roughly with the number of stars (N), the relaxation time becomes <1 Myr for small N systems and shorter than the crossing (or dynamical) time (e.g., Spitzer & Hart 1971). Such a cluster may be unable to attain virial equilibrium and may disperse over a few crossing times. Recent estimates for the minimum number of stars necessary for a stellar system to evolve slowly and have a significant fraction of the stars remain bound is N~100 stars (see Adams & Myers 2000; Adams, this volume). Smaller groups will be identified as stellar aggregates and larger groups as rich clusters.

2. Cluster Membership

Because young clusters are intimately associated with both circumstellar and intracluster dust, infrared observations are essential in establishing cluster membership (see Fig. 1). The membership of clusters can be estimated in a statistical sense by comparing the distribution of infrared magnitudes with that of a reference field off the cloud that is artificially reddened. J- and K-band luminosity functions have also been useful in looking for variations in the star-forming histories and underlying mass functions between star-forming regions (e.g., Lada & Lada 1995; Muench, Lada, & Lada 2000).

Alternatively, YSOs in a cluster can be identified individually through a variety of observations. Due to the long contraction timescales for low mass stars, no single wavelength band is sufficient to sample completely the cluster members. As shown in Fig. 2, the emergent flux from a YSO is dominated by cool dust in the most deeply embedded Class 0 or Class I phase, making the optimum wavelengths of observation the millimeter or far-infrared bands. Strong stellar winds also mark this phase of evolution and they can be detected through observations of radio continuum emission from ionized gas, high-velocity molecular gas, or shocked molecular hydrogen. YSOs which have dissipated their cool dust envelopes are often optically visible and said to be in a Class II phase which includes Classical T Tauri stars (CTTS). The presence of a strong near-infrared excess indicates the presence of an optically-thick circumstellar disk characteristic of these more evolved objects. Optical and infrared spectroscopic

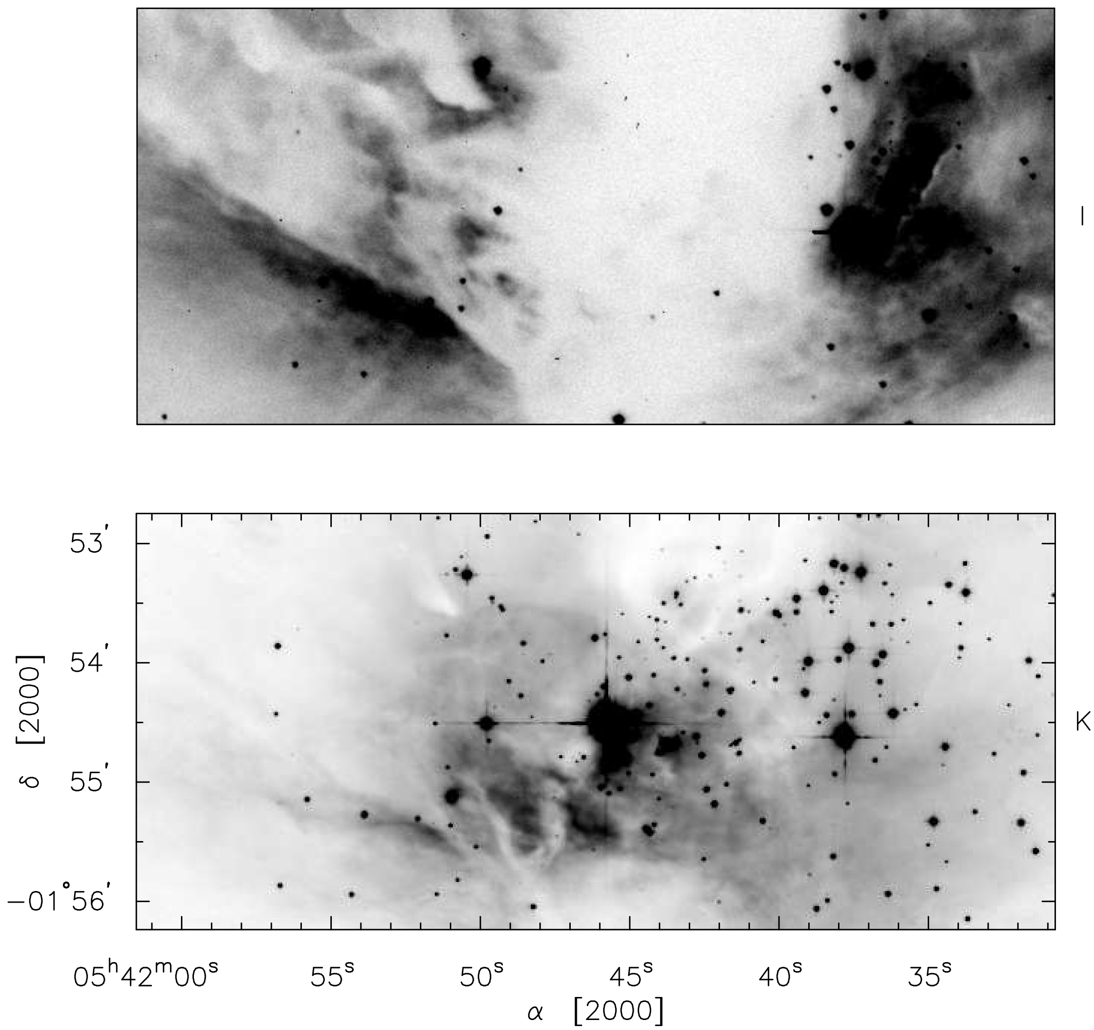

Figure 1. Images of the NGC 2024 cluster in the I-band (top panel) and in K′ (bottom panel). The I-band image was obtained by P. Hartigan with the KPNO 0.9-m telescope and has a completeness limit of I=18 mag. The K′ image is from Hodapp (1994) and was obtained with the UH 2.2-m telescope. It has a completeness limit of 16.5 mag. The figure is courtesy of J. Carpenter and M. Meyer.

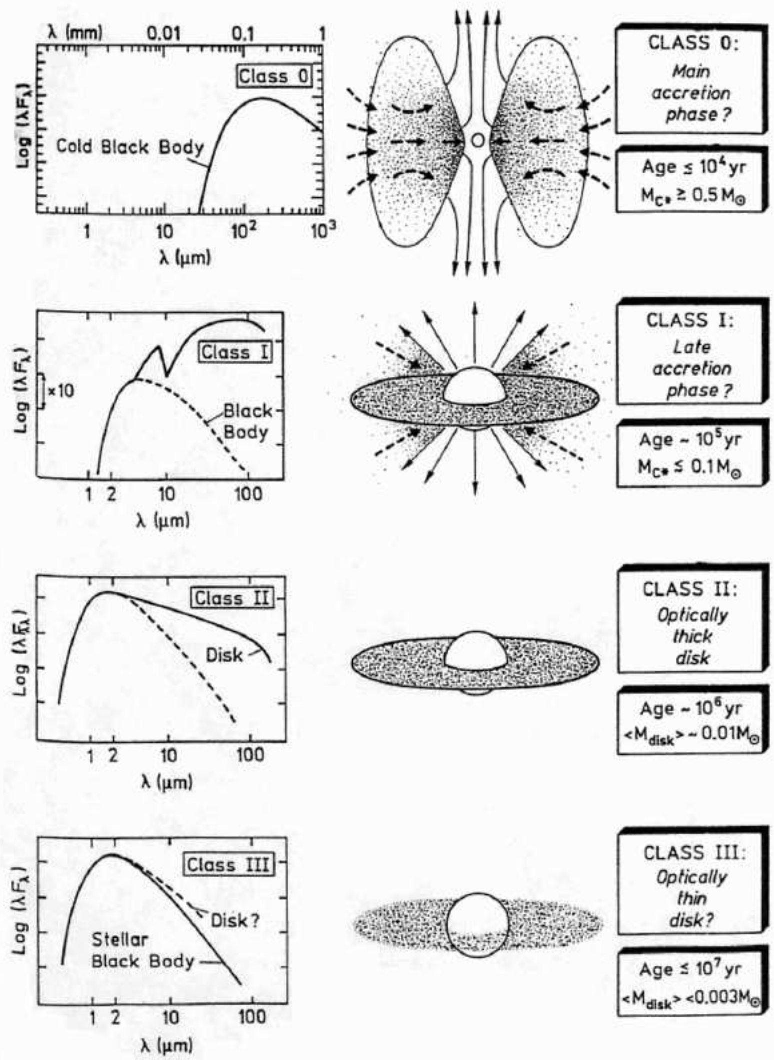

Figure 2. The different stages in the evolution of a low mass star. The earliest Class 0 phase is shown at the top of the figure, followed by Class I, Class II (including CTTS), and Class III (bottom). A spectral energy distribution characteristic of each stage is shown on the left and indicates the optimum wavelengths for observation. The figure is from André (1994).

surveys, including emission-line surveys, are also efficient ways to classify Class II objects. Once the YSOs have dissipated most of their circumstellar dust, they are difficult to distinguish from field stars. Yet magnetic surface activity in these Class III objects produces x-ray and radio continuum emission that is readily observed. Optical spectroscopy and Li absorption are other techniques used to identify Class III YSOs.

3. Observable Cluster Properties

A number of cluster properties can be obtained directly from observations. First, young clusters are associated with dense ($>10^4$ cm^{-3}) molecular gas. A good example is the L1630 region where an unbiassed CS survey revealed 42 molecular cores with infrared clusters associated with the four most massive clumps (E. Lada et al. 1991). Next, young clusters are more compact than exposed open clusters, with effective radii ranging from 0.1 pc–1 pc. This compactness underscores their close assocation with molecular gas. Young clusters generally lack spherical symmetry and often mimic the distribution of dense molecular gas in which they are embedded (e.g., ρ Oph, NGC 1333). There is a tendency in rich clusters and in aggregates with massive stars (>3 M$_\odot$) to have these stars located near the cluster center (e.g., the R Cr A and BD+40°4124 aggregates). Because rich clusters such as the ONC are too young to have undergone dynamical mass segregation, it has been suggested that the massive stars formed near the cluster center (Bonnell & Davies 1998).

3.1. Stellar Density

Table 1 summarizes the radii, number of cluster members, and stellar densities for a collection of well-studied young clusters within 1 kpc of the Sun. In general, the boundaries of these young clusters have been defined by near-infrared observations. However we note that deep x-ray surveys of dense cores have not only revealed a more extensive distribution of PMS stars (e.g., Walter et al. 2000) but also a population of low-luminosity PMS objects not sampled by near-infrared observations (Garmire et al. 2000). The completeness limit of the λ=2.2 μm survey used to identify cluster members, K$_{lim}$ in magnitudes, is given in column 8. Column 9 gives the depth of the cloud layer (in magnitudes of visual extinction) that is completely sampled for YSOs at or above the hydrogen-burning limit assuming an age of 1 Myr and the DM (1998) models. Clearly, these infrared surveys are sensitive to brown dwarfs which reside within this layer. While there are uncertainties due to a spread in the YSO ages, Table 1 shows that the memberships of clusters with d$\leq$310 pc are complete for YSOs above the hydrogen-burning limit through a substantial fraction of the cloud and will contain brown dwarfs. Of the more distant regions, only the central regions of the ONC, NGC 2024, Mon R2 and LkHα 101 have been probed to such depths.

The stellar density for the stellar system as a whole, in units of stars pc^{-3}, is given in column 5. The stellar density for this sample ranges from 13–7400 stars pc^{-3} with a median value of 150 stars pc^{-3}. The inferred stellar mass densities are at least an order of magnitude greater than the value needed for stablilty against tidal disruption by passing clouds and than the stellar mass densities of exposed open clusters. For example, the Pleiades cluster has a stellar mass density of 2 $M_\odot$ pc^{-3}. The additional binding mass of the molecular gas is responsible for the higher densities of young clusters. There is no discernable difference between the overall stellar densities of aggregates and rich clusters.

However, this is a marked difference between the stellar densities of aggregates vs. rich clusters if one considers only the stellar density within R=0.15 pc of the cluster center. As shown in column 7, rich clusters show a much higher degree of central concentration with a median stellar density of 6000 stars pc^{-3} compared to a value of 1000 stars pc^{-3} for aggregates. The central regions of the ONC reach a stellar density of 17000 stars pc^{-3}! It is a general property of rich clusters that the cluster richness is a function of the mass of the most massive star (Hillenbrand 1995; Testi, Palla, & Natta 1999).

3.2. Disk Frequency

The presence of an optically thick circumstellar disk which marks the Class I and Class II phase is most easily detected at mid-infrared wavelengths. ISOCAM surveys of nearby clouds have provided the most complete samples of Class II objects with passive disks which reprocess stellar photons (see Kaas & Bontemps, this volume and Oloffson et al. 1999; Persi et al. 2000; Bontemps et al. 2000). The presence of an active accretion disk surrounding a YSO can be determined by observational signposts such as an ultraviolet excess, broad Hα or Ca II emission, spectral veiling, or a near-infrared excess. Near-infrared arrays have provided complete samples of YSOs with active accretion disks in star-forming regions covering a wide range of distances. By plotting the YSOs in a $(J-H)$ vs. $(H-K)$ diagram, the disk frequency in a young cluster can be established by comparing the YSO colors to that of reddened main sequence dwarfs, giants, and CTTS. As shown in Fig. 3 for the NGC 2024 cluster, YSOs which fall within the reddening band of CTTS have excess emission at K due to warm, circumstellar dust. Spectroscopic studies of the Taurus-Auriga cloud indicate that only of 2/3 of CTTS show a clear excess in a $(J-H)$ vs. $(H-K)$ diagram; about 1/3 of the CTTS lie within the reddening band for main sequence stars yet have K excesses relative to their main sequence colors (Meyer, Calvet, & Hillenbrand 1997).

With this correction factor in mind, the fraction of K excess sources in a young cluster can be estimated. Ideally, one estimates this fraction for an extinction-limited sample determined from a color-magnitude diagram using colors and reddening laws from a common photometric system. For the clusters shown in Table 1, the disk frequencies are estimated to be 20%–60% from the $(J-H)$ vs. $(H-K)$ diagram alone. If these clusters are similar to the CTTS in Taurus-Auriga, the true disk frequencies range from 30%–90% with a median value of 50%. Given that there is evidence for variations in reddening laws between clouds (Wilking et al. 1997) and that the young clusters in Table 1 all very similar in age (0.3–3 Myr), it is not possible to explore potential variations of the disk frequency with cluster age or stellar density for this sample. However for the ONC, a large enough sample is available to investigate the variation of disk frequency with stellar mass and stellar density (cluster radius). For the ONC, Hillenbrand et al. (1998) find that the disk frequency does not drop to-

Table 1. **Summary of Young Cluster Properties**

Name	Dist. (pc)	R_{eff}[a] (pc)	N_* ($R=R_{eff}$)	Density[b] ($R=R_{eff}$)	N_* (R=0.15 pc)	Density[b] (R=0.15 pc)	K_{lim}[c]	A_v[d]	Ref.[e]
R Cr A	130	0.28	22	240	12	850	16.5	65	(1)
ρ Oph	150	0.35	105	580			15.5	50	(2)
ρ Oph A	150				35	2500	16	56	(3)
NGC 1333	300	0.50	110	210			13.5	11	(4)
NGC 1333S	300				18	1300	16.2	41	(5)
IC 348	300	1.00	330	80	30	7200	13.5	11	(6)
Serpens	310	0.22	55	1200			16.3	42	(7)
CK Group	480	0.66	25	21	10	710	14.8	14	(8)
L1641N	480	0.66	43	36	15	1100	14.8	14	(8)
V380 Ori	480	0.86	34	13	8	570	14.8	14	(8)
L1641S	480	1.30	134	15	17	1200	14.8	14	(8)
NGC 2023	480	0.30	21	190			13	0	(9)
NGC 2024	480	0.88	309	110			13	0	(9)
	480				120	8500	16	28	(10)
NGC 2068	480	0.86	192	70			13	0	(9)
NGC 2071	480	0.59	105	120			13	0	(9)
ONC	480	2.50	3500	50			...	2	(11)
	480	0.39	647	2600	238	17000	17.5	44	(12)
S106	600	0.30	160	1400	82	5800	14	0	(13)
LkHα 101	800	0.08	17	7400	17	7400	16.8	24	(14)
Mon R2	830	0.86	475	180			14.5	0	(15)
	830				95	6700	16.6	21	(15)
BD+40°4124	980	0.36	33	170	26	1800	15.3	3	(16)

[a] The cluster radius is either the observed radius or, for irregularly shaped groups, $\sqrt{A/\pi}$ where A is the project cluster area.

[b] Stellar density in units of stars pc^{-3}.

[c] Completeness limit at λ=2.2 μm.

[d] The depth of the cloud layer that is completely sampled for YSO masses $M<0.08\ M_\odot$ assuming an age of 1 Myr. The absolute K magnitude given by the DM (1998) models for this mass and age is M(K)=5.1.

[d] References for data: (1) Wilking *et al.* (1997); (2) Comerón *et al.* (1993); (3) Wilking *et al.* (2000); (4) C. Lada, Alves, & E. Lada (1996); (5) Aspin, Sandell, & Russell (1994); (6) E. Lada & C. Lada (1995); (7) Giovannetti *et al.* (1998); (8) Allen & Hillenbrand (1999); (9) E. Lada *et al.* (1991); (10) Meyer *et al.* (2000); (11) Hillenbrand (1997); (12) Hillenbrand & Carpenter (2000); (13) Hodapp & Rayner (1991); (14) Aspin & Barsony (1995); (15) Carpenter *et al.* (1997); (16) Hillenbrand, Meyer, & Strom (1995)

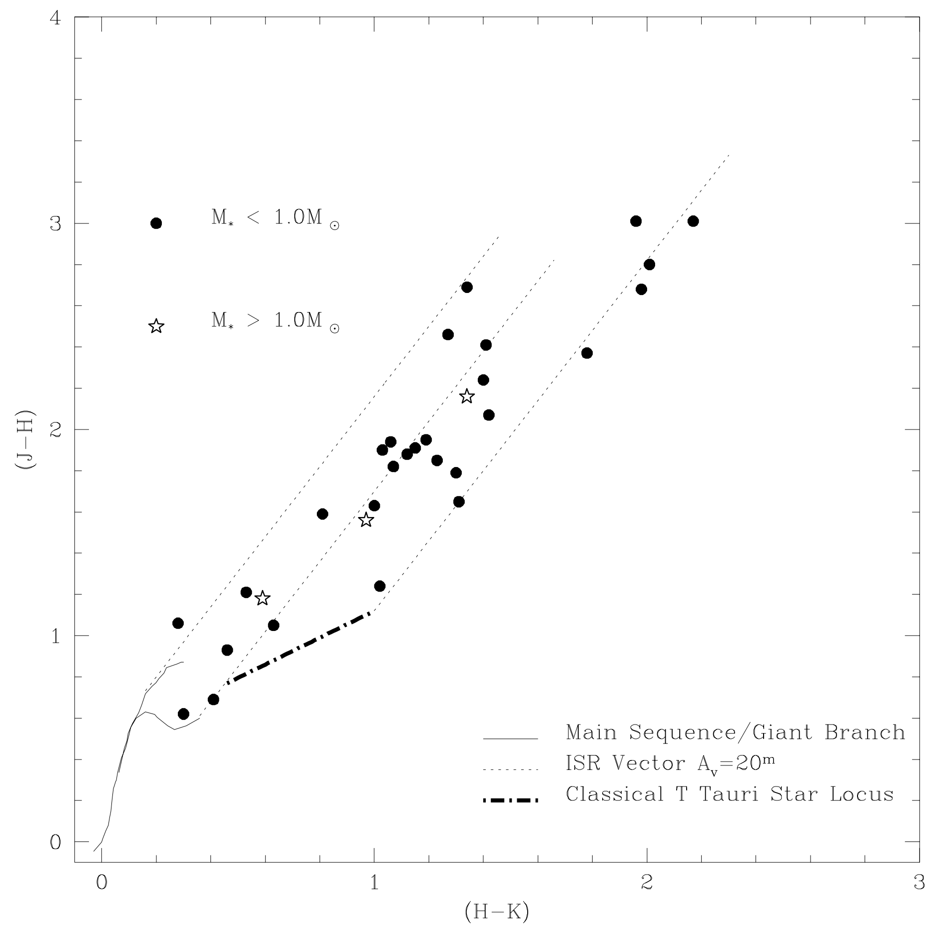

Figure 3. A color-color diagram for the NGC 2024 infrared cluster pictured in Fig. 1. The locus of unreddened CTTS is shown by the dot-dashed line. Reddening vectors representing standard interstellar reddening of $A_v = 20$ mag are shown by the dashed lines (Meyer et al. 2000). Objects within the reddening band for CTTS clearly have active accretion disks.

ward the cluster center where stellar densities are greatest but does decrease with decreasing stellar mass.

3.3. Binary Frequency

The frequency of binary stars in clusters must be established using a variety of observational techniques. As shown in Table 2, different techniques probe different projected separations. The approximate range of projected separations covered by each technique is given in both angular units (column 2) and linear units (column 3). References that provide representative examples of the application of the technique are given in the last column. Estimates of the companion star fractions in rich clusters for projected separations of 10–2000 AU are found to be comparable to main sequence values independent of age. However there is evidence that the companion star fraction is higher in loose associations such as that in Taurus-Auriga cloud (see Duchêne 1999 and this volume).

Table 2. **Detection of Binaries**

Technique	Ang. Sep. ($''$)	Linear Sep. (AU at 150 pc)	Examples[a]
Spectroscopy	0.0002–0.003	0.003–0.45	(1)
Lunar Occultations	0.005–1	0.75–150	(2)
HST Imaging	0.06–2.0	9–300	(3),(4)
Speckle Imaging	0.1–1.8	15–270	(5)
Adaptive Optics Imaging	0.3–1.0	50–150	(6)
Direct Imaging	0.8–12	120–1800	(7)

[a]Examples of technique include: (1) Mathieu, Walter, & Myers (1989); (2) Simon *et al.* (1995); (3) Prosser *et al.* (1994); (4) Padgett, Strom, & Ghez (1997); (5) Ghez *et al.* (1993); (6) Simon, Close, & Beck (1999); (7) Reipurth & Zinnecker (1993)

4. Ages and Masses of Cluster Members

Due to the recent availability of multi-object spectrographs for optical astronomy and infrared spectrographs, the distributions of masses and ages within young clusters can now be explored in detail. The masses and ages of individual cluster members can be estimated by comparing their luminosities and effective temperatures to evolutionary models for PMS stars on a Hertzsprung-Russell diagram. Since the surface gravities of PMS stars are more similar to those of main sequence dwarfs than giants (e.g., Greene & Lada 1997), effective temperatures are derived from spectra by adopting a temperature scale appropriate for dwarfs or subgiants. Luminosities are typically derived by dereddening the J- or H-band magnitudes and applying the appropriate bolometric corrections.

Using similar sets of theoretical PMS tracks and isochrones, significant differences in relative ages in young clusters is evident. The mean ages derived from the models of D'Antona & Mazzitelli (DM 1994, 1997) yield ages which vary from $\sim$0.3 Myr for the ρ Oph and NGC 2024 clusters (Greene & Meyer 1995; Luhman & Rieke 1999; Bontemps et al 2000; Meyer et al. 2000) to $\sim$3

Myr for the L1641S and IC 348 clusters (Allen & Hillenbrand 1999; Luhman et al. 1998). Fig. 4 shows a set of H-R diagrams for the IC 348 cluster (Luhman et al. 1998). The cluster has a mean age of 3 Myr with the youngest objects near the cluster center (see also Herbig 1998). Like most clusters of comparable age, a spread in ages from 0.5 Myr to 10 Myr is observed. All YSOs with strong disk signatures (bottom panel) are <3 Myr old suggesting a shorter disk survival timescale in IC 348 compared to Taurus-Auriga.

Investigating the mass functions of young clusters has distinct advantages over similar studies in exposed clusters. Contamination by background stars is minimized due to the compactness of the cluster and the obscuration provided by the molecular cloud. The youth of the cluster removes the need for corrections for post-main sequence evolution and for cluster evaporation. The mass function at the lowest masses is also more complete since very low mass and substellar objects are much more luminous in their youth due to deuterium burning. Finally, any variations observed in the mass function can be directly related to the physical conditions of the associated molecular gas. An obvious disadvantage is the reliance of the mass estimates on the adopted set of PMS models.

The key questions to be addressed in these studies are whether the slope of the mass function rises or falls toward the brown dwarf regime and whether one can observe variations in the mass function at low masses between clusters. Techniques used to study mass functions include modeling of J- or K-band luminosity functions (e.g., Muench et al. 2000), or deriving masses for individual YSOs using multi-color infrared photometry (e.g., Comerón Rieke, & Rieke 1996), optical and/or infrared spectroscopy (Hillenbrand 1997; Luhman et al 1998), combined spectroscopic and photometric data (see chapters by Hillenbrand and by Luhman, this volume).

Mass functions derived from spectroscopic and photometric data are now available for several young clusters and are described in more detail elsewhere in this volume. For the ONC and IC 348 clusters, these mass functions are complete down to 0.02 $M_{\odot}$ or 20 Jupiter masses (Hillenbrand & Carpenter 2000; Luhman et al. 2000; Najita, Teide, & Carr et al. 2000). Briefly, using the same set of PMS models, the mass functions in dark clouds and giant molecular clouds are surprisingly similar. They appear to be flat or slowly rising from substellar masses to a peak in the range of 0.15–0.4 $M_{\odot}$ for DM models. Using logarithmic units where $dN/dlogM \propto M^{\Gamma}$, the slopes of the mass function at low masses vary from 0.4 to 0.6. (For comparison, the slope at high masses derived by Salpeter (1955) was Γ = -1.35.) This is consistent with the slope derived for the Pleiades cluster at low masses of Γ = 0.4 (Bouvier et al. 1998) but inconsistent with the slope derived from field stars. Comparing L-dwarf surface densities and temperature distributions with that observed by the DENIS and 2MASS surveys, Reid et al. (1999) derive a substellar mass function for field stars which is flat or rises slightly toward lower masses (Γ = 0 to -1). It should be noted that the precise shape of the mass function depends on the set of PMS models used. In any case, it is clear that while brown dwarfs are numerous in the young clusters studied thus far, they do not contribute significantly to the total cluster mass.

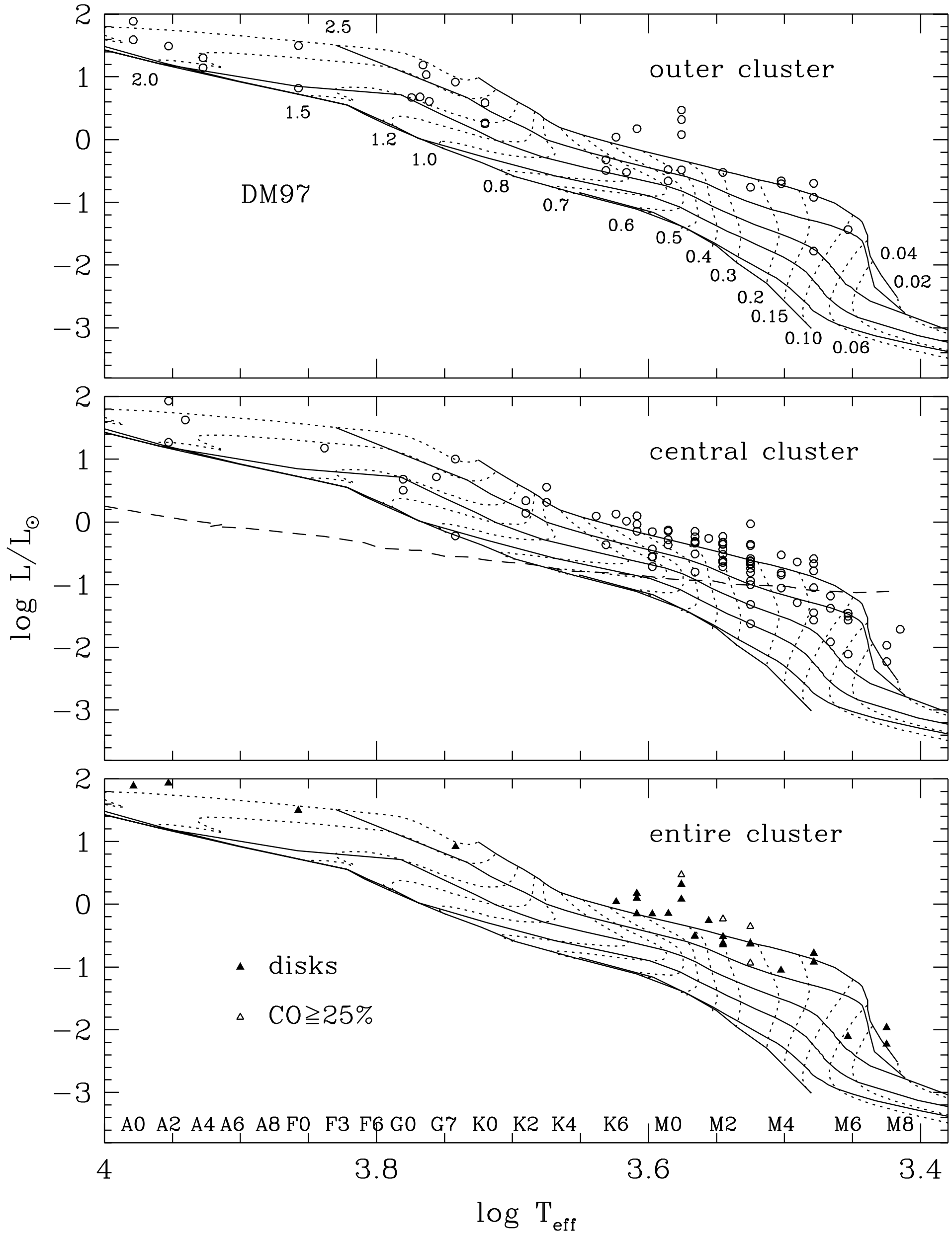

Figure 4. H-R diagrams for the IC 348 cluster using the PMS models of DM (1997). The middle panel shows the H-R diagram for the central cluster compared to diagrams for sources outside the center (top) and sources with strong disk signatures. Dashed lines mark mass tracks from 0.02 $M_\odot$ to 2.0 $M_\odot$ which are labeled in the top panel. Solid horizontal lines mark isochrones for ages from top to bottom of 1, 3, 10, 30, and 100 Myr. The figure is from Luhman et al. (1998).

5. The Fates of Young Clusters

It is clear that the majority of young embedded clusters will not evolve into gravitationally bound exposed clusters. Instead it is expected that as they emerge from their molecular clouds, most of these clusters will disperse and dissolve into the field. Following the arguments presented by Lada & Lada (1991), we assume an average of three embedded clusters per GMC and an average age of 5 Myr. Given that there are about 12 GMCs within 2 kpc of the Sun, this yields a birthrate of clusters of 7×10^{-6} clusters yr^{-1}. Given a constant birthrate, this would predict that ∼700 visible clusters have formed over the past 100 Myr within 2 kpc of the Sun. However, only 94 exposed clusters are observed (Elmegreen & Clemens 1985) and this is an upper limit to the number of bound clusters since some of the younger clusters included in this sample may be unbound. Hence, only about 10% of embedded clusters evolve into gravitationally bound exposed clusters. Since only 10% of the field stars have their origins in gravitationally bound open clusters (Roberts 1957; Miller & Scalo 1978), this implies that 90% of the field stars come from the dispersal of embedded clusters and the distributed populations in GMCs. It has been suggested that the majority of field stars form in poor clusters containing 10–100 stars (Adams & Myers 2000).

The question then becomes: which embedded clusters will produce gravitationally bound open clusters? Estimates for the star formation efficiency in young clusters range from η = 20%–40% where $\eta = \mathrm{M}_{stars}/(\mathrm{M}_{stars} + \mathrm{M}_{gas})$ (e.g., Lada & Lada 1991). For the richest cluster in the solar neighborhood, the ONC, $\eta \approx 40\%$ (Hillenbrand & Hartmann 1998). It is important to note that the star formation efficiency is a time-dependent quantity and will continue to increase in regions not disrupted by massive stars. Analytical models indicate that for young clusters which rapidly dissipate their molecular gas, η must be greater than 50% for the formation of a bound cluster. However, if the molecular gas is released on a timescale much greater than the crossing time, then η need only exceed 30% for the cluster to remain bound (e.g., Elmegreen 1983; Mathieu 1983; Vershueren & David 1989). More sophisticated semi-analytical and numerical models do allow clusters which rapidly dissipate their molecular gas to form bound systems with $\eta < 50\%$, but this is accompanied by a loss of a significant fraction (>20%) of its stars (Lada, Margulis & Dearborn 1984; Adams 2000)

Acknowledgments. I would like to thank Lori Allen, John Carpenter, and Lynne Hillenbrand for communicating data in advance of publication and to Philippe André, John Carpenter, Kevin Luhman, and Michael Meyer for providing figures. I also thank Michael Meyer for many helpful discussions.

References

Adams, F. C. 2000, ApJ, in press

Adams, F. C. & Myers, P. C. 2000, submitted to ApJ

Allen, L. & Hillenbrand, L. 1999, to appear in the ASP Conference Series, The Orion Complex Revisted, eds. M.J. McCaughrean and A. Burkert

André, Ph. 1994 in the Cold Universe, eds. T. Montmerle, C. Lada, I. Mirabel, & J. Tran Thanh (Gif-sur-Yvette: Editions Frontiéres), p. 179

Aspin, C. & Barsony, M. 1995, A&A, 288, 849

Aspin, C., Sandell, G., & Russell, A. 1994, A&AS, 106, 165

Bonnell, I. A. & Davies, M. B. 1998, MNRAS, 295, 691

Bontemps, S., André, P., Kaas, A. et al. 2000, A&A, in press

Bouvier, J., Stauffer, J., Martín, E., Barrado y Navascués, D., Wallace, B., & Bejar, V. J. 1998, A&A, 336, 490

Carpenter, J., Meyer, M., Dougados, K., Strom, S., & Hillenbrand, L. 1997, AJ, 114, 198

Comerón, F., Rieke, G., Burrows, A., & Rieke, M. 1993, ApJ, 416, 185

Comerón, F., Rieke, G., & Rieke, M. 1996, ApJ, 473, 294

D'Antona, F. & Mazzitelli, I. 1994, ApJS, 90, 467

D'Antona, F. & Mazzitelli, I. 1997, in Cool Stars in Clusters and Associations, eds. R. Pallavicini & G. Micela, Mem. S. A. It., 68, n.4.

D'Antona, F. & Mazzitelli, I. 1998, private communication

Duchêne, G. 1999, A&A. 341, 547

Elmegreen, B. 1983, MNRAS, 203, 1011

Elmegreen, B. & Clemens, C. 1985, ApJ, 294, 523

Garmire, G., Feigelson, E., Broos, P., Hillenbrand, L., Pravdo, S., Townsley, L., & Tsuboi, T. 2000, ApJ, 120, 1426

Ghez, A., Neugebauer, G., & Matthews, K. 1993, AJ, 106, 2005

Giovannetti, P. Caux, E., Nadeau, D., Monin, J.-L. 1998, A&A, 330, 990

Greene, T. P. & Lada, C. J. 1997, AJ, 114, 2157

Greene, T. P. & Meyer, M. 1995, ApJ, 405, 233

Herbig, G. H. 1998, ApJ, 497, 736

Hillenbrand, L. 1995, Ph.D. Thesis, University of Massachusetts

Hillenbrand, L. 1997, AJ, 113, 1733

Hillenbrand, L. & Carpenter, J. 2000, ApJ, in press

Hillenbrand, L. & Hartmann, L. 1998, ApJ, 492, 540

Hillenbrand, L., Meyer, M., & Strom, S. 1995, AJ, 109, 280

Hillenbrand, L., Strom, S., Calvet, N., Merrill, K., Gatley, I., Makidon, R., Meyer, M., & Skrutskie, M. F. 1998, AJ, 116, 1816

Hodapp, K.-W. & Rayner, J. 1991, AJ, 102, 1108

Lada, C. J., Alves, J., & Lada, E. A. 1996, AJ, 111, 1964

Lada, C. J. & Lada, E. A. 1991, in the Formation and Evolution of Star Clusters, ed. K. A. Janes (San Francsico: ASP), 3

Lada, C. J., Margulis, M., & Dearborn, D. 1984, ApJ, 285, 141

Lada, E. A., Depoy, D. L., Evans, N. J., II, & Gatley, I. 1991, ApJ, 371, 171

Lada, E. A. & Lada, C. J. 1995, AJ, 109, 1682

Leisawitz, D., Bash, F. & Thaddeus, P. 1989, ApJS, 70, 731

Li, W., Evans, N. J., & Lada, E. A. 1997, ApJ, 488, 277

Luhman. K. & Rieke, G. 1999, ApJ, 525, 440

Luhman. K., Rieke, G., Lada, C., & Lada, E. 1998, ApJ, 508, 347

Luhman. K., Rieke, G., Young, E., Cotera, A., Chen, H., Rieke, M., Schneider, G., & Thompson, R. 2000, ApJ, in press

Mathieu, R. 1983, ApJ, 267, L97

Mathieu, R., Walters, F., & Myers, P. 1989, AJ, 98, 987

Meyer, M., Calvet, N., & Hillenbrand, L. 1997, AJ, 114, 288

Meyer, M., Carpenter, J., Strom, S., Hillenbrand, L., & Skrutskie, M. 2000, submitted to AJ

Meyer, M. R. & Lada, E. A. 1999, to appear in the ASP Conference Series, The Orion Complex Revisted, eds. M.J. McCaughrean and A. Burkert

Miller, G. & Scalo, J. 1978, PASP, 90, 506

Muench, A. A., Lada, E. A. & Lada, C. J. 2000, ApJ, 533, 358

Najita, J., Tiede, G., & Carr, J. 2000, ApJ, in press

Oloffson, G., Huldtgren, M., Kaas, A. et al. 1999, A&A, 350, 883

Padgett, D., Strom, S., & Ghez, A. 1997, 477, 705

Persi, P., Marenzi, A. R., Oloffson, G. et al. 2000, A&A, 357, 219P

Prosser, C., Stauffer, J., Hartmann, L., Soderblom, D., Jones, B., Werner, M., & McCaughrean, M. 1994, ApJ, 421, 517

Reid, I. N., Kirkpatrick, D., Liebert, J., Burrows, A., Gizis, J., Burgasser, A. Dahn, C., Monet, D., Cutri, R., Beichman, C., & Skrutskie, M. 1999, ApJ, 521, 613

Reipurth, B. & Zinnecker, H. 1993, A&A, 278, 81

Roberts, M. 1957, PASP, 69, 59

Salpeter, E. E. 1955 ApJ, 121, 161

Simon, M., Close, L., & Beck, T. 1999, AJ, 117, 1375

Simon, M., Ghez, A., Leinert, Ch., Cassar, L. Chen, W.-P., Howell, R., Jameson, R., Matthews, K., Neugebauer, G., & Richichi, A. 1995, ApJ, 443, 625

Spitzer, L. 1958, ApJ, 127, 17

Spitzer, L. & Hart, M. 1971, ApJ, 164, 399

Testi, L., Palla, F., Natta, A. 1999, A&A, 342, 515

Vershueren, W. & David, M. 1989, A&A, 219, 105

Walter, F. M., Alcalá, J. M., Neuhäuser, R., Sterzik, M., & Wolk, S. J. 2000, in Protostars and Planets IV, eds. V. Mannings, A. P. Boss, and S.S. Russell, (Tucson: Arizona Press), p. 273

Wilking, B., McCaughrean, M., Burton, M., Giblin, T., Rayner, J., & Zinnecker, H. 1997, AJ, 114, 2029

Wilking, B., Greene, T. & Meyer, M. 2000, in preparation